Journal of Modern Optics

Polarization dependence on downconversion emission angle: investigation of the 'Migdall effect'

Radhika Rangarajan [a], Alfred B. U'Ren [b] & Paul G. Kwiat [a]

[a] Department of Physics, University of Illinois at Urbana-Champaign, 1110 W Green St., Urbana, IL 61801, USA

[b] Instituto de Ciencias Nucleares, Universidad Nacional Autónoma de México, Apartado Postal 70-543, 04510 DF, Mexico City, Mexico
Published online: 20 Sep 2010.

PLEASE SCROLL DOWN FOR ARTICLE

Taylor & Francis
Taylor & Francis Group

Polarization dependence on downconversion emission angle: investigation of the 'Migdall effect'

Radhika Rangarajan[a]*, Alfred B. U'Ren[b] and Paul G. Kwiat[a]

[a]*Department of Physics, University of Illinois at Urbana-Champaign, 1110 W Green St., Urbana, IL 61801, USA;*
[b]*Instituto de Ciencias Nucleares, Universidad Nacional Autónoma de México, Apartado Postal 70–543, 04510 DF, Mexico City, Mexico*

Photonic sources based on spontaneous parametric downconversion (SPDC) are now pervasively employed in optical quantum information processing protocols. The recent focus on engineering efficient photonic sources requires a thorough understanding of several of the subtler characteristics of SPDC, which had previously been negligible. Here, we experimentally investigate one such phenomenon – the dependence of the downconversion polarization on emission angle. Additionally, we discuss the significance of this effect from the perspective of better engineering SPDC sources. We also propose techniques, specifically in the context of a two-crystal scheme for generating polarization-entangled photons, to exploit the effect and drastically improve source quality in certain limiting cases.

1. Introduction

Photons produced via the nonlinear process of spontaneous parametric downconversion (SPDC) are now routinely used in a vast array of experiments, from fundamental tests of quantum mechanics, to quantum cryptography and teleportation, to implementing small quantum algorithms. Recently, there has been an increased focus on developing highly efficient photonic sources by engineering the emitted quantum state, both simple (e.g. pure) and complex (e.g. polarization entangled), at the source. To optimally design efficient sources, we require in-depth understanding of previously negligible effects, some of which may become dominant as the underlying parameter space expands. One such effect is the variation in the downconversion polarization orientation along the emission cone of a non-collinear SPDC source, first predicted by A. Migdall in 1997 [1], and here labeled as the 'Migdall effect'. In type-I phase-matching in negatively uniaxial crystals[1], the pump is extraordinary polarized while both the downconversion photons are ordinary polarized. Thus, the downconversion polarization, whilst being ordinary everywhere, is no longer orthogonal to the pump polarization, except at certain specific locations. The Migdall effect becomes especially noticeable when the emission angles become significant compared with the crystal optic axis tilt.

Further, the variation in downconversion polarization is accompanied by a corresponding inhomogeneity in the nonlinear conversion efficiency, a second subtle effect that cannot be ignored while designing efficient sources [1].

While a few experiments/proposals (for example [2,3]) have been wary of the Migdall effect, it has, to our knowledge, thus far never been experimentally verified; in most experiments, the effect is insignificant for two main reasons. First, when working with only a single SPDC crystal, one can always collect at specific angles on the cone where the emitted polarization is perpendicular to the pump polarization. Second, even in more complicated setups, the downconversion emission angles under consideration are fairly small ($\sim 3°$), thereby strongly limiting the magnitude of the Migdall effect. In certain cases, however, the effect can dominate the photon-pair state produced. In particular, recent SPDC schemes for engineering photon-pair states exploit group-velocity matching (GVM), in addition to phase-matching (PM) [4,5]. Such state-engineering schemes can then be combined with methods for generating polarization entanglement to create ideal sources for optical quantum information processing [6]. Depending on the SPDC crystal and wavelength regimes of interest, simultaneous GVM and PM occur at larger (than typical) downconversion

emission angles. For instance, generating GVM frequency-degenerate SPDC photon pairs, centered at 810 nm using a β-barium borate (BBO) crystal, requires a crystal optic axis tilt of $\Theta = 40.7°$ [5], which results in a significantly larger external emission half-angle of 16°, compared with the typical $\sim 3°$ cone [7]. In such regimes, the Migdall effect becomes significant. Here, we present the first reported experimental verification of the Migdall effect. Additionally, we discuss novel techniques to counteract this effect in cases where it cannot be easily avoided, e.g. the two-crystal geometry for generating polarization entanglement.

2. Experimental confirmation of the Migdall effect

Naively, for type-I SPDC, we might expect the down-conversion polarization to be $90°_p$,[2] i.e. orthogonal to the incident pump polarization. The Migdall effect predicts the polarizations of the downconverted photons to vary with the emission angles, both with the cone opening half-angles as well as with the azimuthal angles (i.e. around the emission cone). The complete theory can be found in [1]. Figure 1 shows the coordinate system defining these angles, along with a cartoon representation of the Migdall effect. In brief, the origin
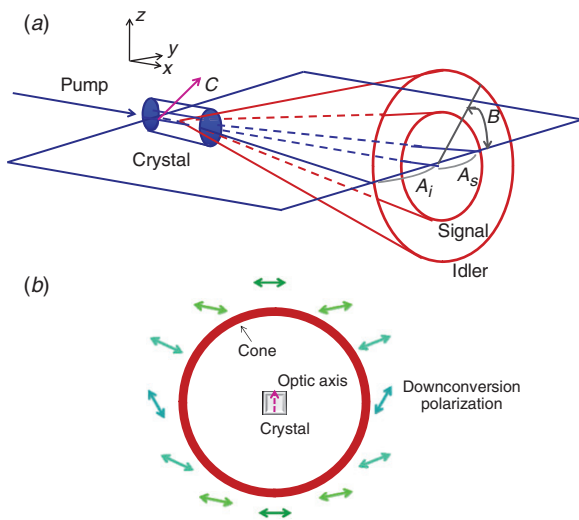
of the effect can be understood as follows. In type-I phase-matching, the downconversion photons are ordinary polarized (assuming a negative uniaxial crystal, like BBO), i.e. their polarization P is perpendicular to both their propagation direction k and the crystal optic axis C, which is inclined at angle Θ with respect to the pump propagation direction, such that:

$$\widehat{P}(A, B) = \widehat{k} \times \widehat{C}(\Theta) \tag{1}$$

where A is the cone half-opening angle, B is the azimuthal emission angle and C is the direction of the optic axis. Since the downconversion propagation direction varies along the cone while the crystal optic axis is fixed, the downconversion polarization measured in the laboratory frame of reference must depend on the emission direction, in spite of being ordinary polarized everywhere along the cone (see Figure 2(a)). As shown in [1], a particular coordinate transformation can be useful in determining the angular dependence of the downconversion polarization. First, rotate about the z-axis by ϕ to give the $x' - y' - z'(z' = z)$ frame, then rotate about the y' axis by γ to give the $x'' - y'' - z''(y'' = y')$. Figure 2(b) shows the ϕ, γ, β coordinate system, in which the angle β defines the polarization of the downconversion photon propagating along the (A, B) direction, and:

$$\phi = \tan^{-1}[\tan A \cos B],$$
$$\gamma = \sin^{-1}[\sin A \sin B]. \tag{2}$$

The output polarization angle β can be found from Equation (1) by transforming P and C into the new coordinate system [1], which yields

$$\beta = \tan^{-1}\left[\frac{-\cos \Theta \cos \phi \sin \gamma + \sin \Theta \cos \gamma}{\cos \Theta \sin \phi}\right]. \tag{3}$$

Figure 1. (a) Schematic showing the crystal coordinate system with the pump beam, crystal optic axis C, and signal and idler half-opening angles A_s and A_i, respectively. The azimuthal angle B is referenced to the y direction and goes around the downconversion cone (based on [1]). (b) A cartoon depiction of the Migdall effect: variation of the downconversion polarization at various points along the emission cone, shown end-on. The central dotted arrow indicates the projection of the optic axis (in the x–z plane) on to the z axis. (The color version of this figure is included in the online version of the journal.)

Figure 2. (a) Schematic representation showing the origin of the Migdall effect. The downconversion photons are ordinary polarized, i.e. their polarization must be perpendicular to both the fixed crystal optic axis C and the emission direction k; thus when the emission direction changes $(k \rightarrow k')$ so does the polarization $(\vec{P} \rightarrow \vec{P'})$. (b) ϕ, γ, β coordinate system and the crystal optic axis, cut at angle Θ in the $x - z$ plane. β is the angle between z'' and P in the $x'' - z''$ plane (based on [1]). (The color version of this figure is included in the online version of the journal.)

Equation (3) implicitly gives the downconversion polarization dependence on both emission angles – the cone opening (A) and the azimuthal angle (B). Figure 3 shows this theoretical dependence along with the measured downconversion polarization from a single crystal, relative to the extraordinary pump polarization (defined to be $0°_p$), as a function of the emission azimuthal angle; here we consider degenerate type-I SPDC centered at 810 nm (405 nm pump) using a β-barium borate (BBO) crystal in two cases: the typical $3°$ ($\Theta_{pm} = 29.3°$) opening half-angle and the larger $16°$ (group-velocity matched, $\Theta_{pm} = 40.7°$) case. In the laboratory frame, downconversion photons are collected on opposite sides of the emission cone, conventionally at either 0° and 180°, or at 90° and 270° azimuthal angles. From Figure 3, the downconversion polarization at the latter azimuthal points is always the desired $90°_p$ regardless of the cone opening angle, making these the ideal collection spots on the cone (for systems requiring the downconversion polarization to be orthogonal to that of the pump); these collection points lie in the plane containing the crystal optic axis and the incident pump direction (Figure 1), making the polarization of the ordinary downconversion photons automatically orthogonal to the pump polarization in the lab frame. As we move away from these optimal collection angles, the downconversion polarization deviates from the ideal $90°_p$, with the effect becoming appreciably larger for larger cone opening half-angles: the Migdall effect for a 16°

downconversion cone exhibits up to a $\sim12°_p$ deviation from the expected $90°_p$ polarization, compared with only a $\sim3°_p$ maximum deviation for a 3° cone (Figure 3). Note that the extreme deviations do *not* occur precisely at $B = 0°, 180°$ azimuthal angles.

3. Migdall effect in the two-crystal scheme

The implications of the Migdall effect become extremely significant in the two-crystal scheme [7] for polarization entanglement, which relies on two orthogonally oriented crystals, each pumped by orthogonal pump polarizations, vertical V and horizontal H, to generate nominally orthogonally polarized downconversion photons in the entangled state $|H\rangle|H\rangle + e^{i\phi}|V\rangle|V\rangle$, where the relative phase ϕ is determined by phase-matching constraints, crystal length, etc. In the two-crystal scheme, we have to additionally contend with the Migdall effect in each of the two crystals. In the lab frame, the two-crystal scheme requires specific azimuthal collection angles for each of the crystals (Figure 4). Assume that we collect signal photons at 0° and idler photons at 180° azimuthal angles, labeled according to the frame of crystal-1. Call the collected state $|S_1I_1\rangle$. Similarly, for the second crystal we collect state $|S_2I_2\rangle$ at 90° (signal) and 270° (idler), where now the angles are labeled with respect to the crystal-2 axes. In the lab frame, all four photons[3] – signal and idler from crystal 1 and crystal 2 – are emitted in a single plane (that also contains the pump beam direction). Note that in each crystal the signal and idler are always collected 180° apart because
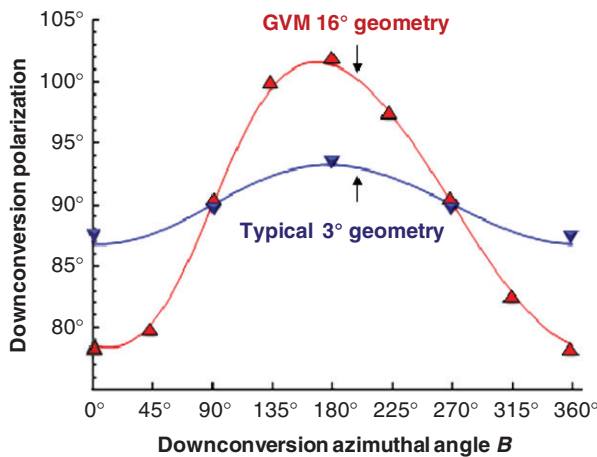

Figure 3. Experimental data (triangles) and theoretical predictions (solid lines) of the Migdall effect, showing the expected downconversion polarization orientation versus azimuthal collection angle for 3° and 16° cone opening half-angles. Polarization of the downconversion photons is measured relative to the pump polarization (0° in the lab frame). The experimental error is smaller than the size of the data markers. (The color version of this figure is included in the online version of the journal.)

Figure 4. End-on view of the downconversion cones from the first (shown in red) and second (shown in green) crystal in the two-crystal scheme. The first (second) crystal is oriented such that a vertically (horizontally) polarized pump downconverts into horizontally (vertically) polarized photons; i.e. the optic axis for the first (second) crystal lies in the vertical (horizontal) plane. The figure shows the typical collection points in the lab frame (i.e. where the detectors are located) and the actual azimuthal angles, measured relative to the optic axis of each crystal, for the signal and idler photons generated in the two orthogonally oriented crystals. (The color version of this figure is included in the online version of the journal.)

the two photons in a given pair are emitted on opposite sides of the cone.

In each crystal, the desired downconversion polarization is $90°_p$, measured relative to the pump polarization in that crystal (defined to be $0°_p$ in that crystal). As seen from Figure 3, at the azimuthal collection angles 90° and 270°, the downconversion polarizations are always perpendicular to the pump. Hence, the polarizations of both the signal and the idler from the second crystal are the desired $90°_p$, because these photons are collected at 90° (signal) and 270° (idler) azimuthal angles (measured with respect to the crystal's optic axis). However, for photons emitted from the first crystal, the Migdall effect for the 16°-engineered geometry results in $78°_p$ for the signal collected at 0° azimuthal angle, and $102°_p$ for the idler collected at 180°. Note that, because of the requisite orthogonal orientation of the crystals in the two-crystal scheme, collecting only at 90° and 270° from both crystals is not an option.[4]

The Migdall effect in the two-crystal scheme has serious consequences on the generated entangled state. Because the crystals are oriented orthogonal to each other, the ideal generated state can be written in the lab frame as the maximally entangled state $|\psi\rangle_{\text{max}} = (|90°_p, 90°_p\rangle + |0°_p, 0°_p\rangle)/\sqrt{2}$, i.e. the relative downconversion polarizations from each crystal are ideally orthogonal. Due to the Migdall effect, however, the emitted two-photon state is instead $|\psi\rangle_{\text{Migdall}} = (|78°_p, 102°_p\rangle + |0°_p, 0°_p\rangle)/\sqrt{2}$. Now, the polarizations produced by the two crystals are no longer orthogonal to each other; more importantly, there is no basis in which they can be written as a maximally entangled state. The fidelity[5] of $|\psi\rangle_{\text{Migdall}}$ with $|\psi\rangle_{\text{max}}$ is ~96%; the predicted concurrence [8] of $|\psi\rangle_{\text{Migdall}}$ is only 90.8%.[6] Additionally, for sources requiring temporal compensation [9], there is a significant component (~3%), quantified by the overlap between the downconversion states generated from the two crystals, that cannot be temporally compensated and therefore experiences unavoidable de-coherence. In such cases, the final predicted maximum concurrence is ~88%.

4. Exploiting the Migdall effect to generate a maximally entangled state

In cases where optimizing the collection angles is not possible, the Migdall effect appears to limit the emitted state quality. However, we propose that we can actually intentionally use the Migdall effect and incorporate it in the two-crystal scheme to generate nearly maximal polarization entanglement, even for larger (e.g. 16°) downconversion emission angles. Our strategy is to collect at nontraditional azimuthal
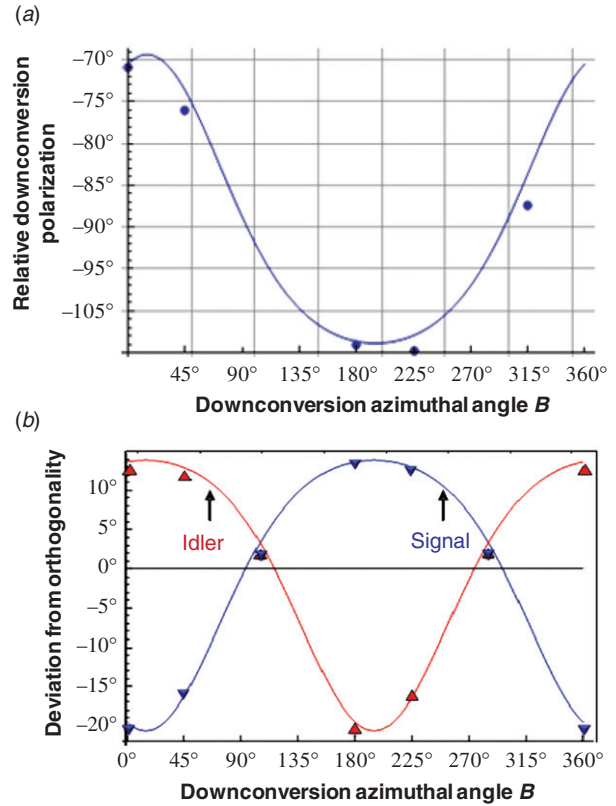

Figure 5. Experimental data (circles/triangles) and theoretical predictions[7] (solid line) for (a). Relative polarization between the downconversion photons – comparing either signals or idlers – from the first and second crystals in the two-crystal scheme, as a function of the location on the downconversion cone, in the reference frame of the lab (ideally, the relative polarization would be ±90°); (b) deviation from perpendicularity between the downconversion photons from the first and second crystals, plotted around the cone for both the signal (collected at B) and idler (at $B + 180°$). The crossing indicates the optimal collection angles $B_o = 105°$ and 285°, for which the downconversion polarizations are the most orthogonal. The experimental error is smaller than the size of the data markers. (The color version of this figure is included in the online version of the journal.)

angles, i.e. locations where the relative polarizations between the downconversion photons generated from the two crystals are almost orthogonal. Figure 5(a) plots the relative polarization between the downconversion photons around the cone, e.g. between the two signal photons. To generate maximally entangled states, we want the relative polarizations to be orthogonal. Further, this needs to be true at two opposite sides of the cone for both the signal and the idler, emitted exactly 180° apart. However, from Figure 5(a) we see that while there are azimuthal locations on the downconversion cone where the two output polarizations are perpendicular, this perpendicularity is not satisfied simultaneously on opposite sides

of the cone, i.e. for both the signal at azimuthal angle B and the idler at $B + 180°$. For example, from Figure 5(a) we see that the two polarizations are exactly perpendicular at $B = 93.6°$ but not so at $B = 93.6° + 180°$. A possible solution is to collect at azimuthal angles for which the deviation from orthogonality is minimized for both the signal and the idler on the downconversion cone. Such a strategy would maximize the overlap with the ideal maximally entangled state $|\psi\rangle_{max} = (|90_p°, 90_p°\rangle + |0_p°, 0_p°\rangle)/\sqrt{2}$. Figure 5(b) plots the deviation from perpendicularity between the polarizations of the downconversion photons generated in the first and second crystals for the signal (at B) and the idler (at $B + 180°$). From this figure, we see that the optimal collection angles are 105° (signal) and 285° (idler), for which the downconversion polarizations between the two crystals deviate from perpendicularity by only $\sim 3°_p$. Hence, the downconversion polarization from the first crystal becomes $93.4°_p$ ($|S_1\rangle$) and $86.6°_p$($|I_1\rangle$), and $0°_p$($|S_2\rangle$) and $0°_p$($|I_2\rangle$) for the second crystal, where we have relabeled the polarization angles.[7] Thus, instead of producing the ideal state $(|90_p°, 90_p°\rangle + |0_p°, 0_p°\rangle)/\sqrt{2}$ from the two crystals, we produce, after local corrections, $(|93.4_p°, 86.6_p°\rangle + |0_p°, 0_p°\rangle)/\sqrt{2}$, which has 99.6% predicted fidelity with a maximally entangled state and a concurrence above 98% (assuming no de-coherence). While the discussion here has been limited to the two-crystal geometry, it might be possible to extend the nontraditional collection angle technique to other schemes where the Midgall effect is non-negligible.

5. Conclusions

As we move towards novel schemes to engineer photon states using spontaneous parametric downconversion, previously ignorable effects become significant and need to be addressed. Here, we have experimentally confirmed for the first time an important SPDC property – the Migdall effect, which refers to the emission and collection angular dependence of the emitted polarizations. The effect becomes especially noticeable when the emission angles become significant compared with the crystal optic axis tilt, as is the case for certain photonic state engineering schemes. To counter the resulting negative impact on the produced photon states in certain cases, e.g. the two-crystal scheme for generating polarization-entangled photons, we have developed a strategy – collecting at nontraditional locations on the downconversion cone – that should mitigate the Migdall effect, thereby broadening the options available for engineering optimal sources for optical quantum information processing.

Notes

1. While the discussion has been presented for type-I phase-matching, both here and in the original paper describing the effect, it can be extended to apply to type-II SPDC, and for other kinds of crystals.
2. The subscript p is used to indicate a polarization angle, to be distinguished from emission/collection angles. The polarization angles are defined with respect to the pump polarization in the SPDC crystal under consideration.
3. In reality we only have a single pair of emitted photons, but with equal amplitudes for it to have originated in either crystal.
4. Collection from both crystals at 90° and 270° azimuthal angles might be possible by inserting a wave plate between two crystals oriented with their optics axis parallel to each other. In both crystals, the horizontally polarized pump downconverts into vertically polarized photons and we collect at 90° and 270° azimuthal angles. The wave plate rotates the downconversion from the first crystal $|V\rangle|V\rangle \rightarrow |H\rangle|H\rangle$, thereby generating a maximally entangled state. Note that the wave plate must be chosen not to rotate the pump wavelength.
5. Fidelity measures the amount of overlap between two states ρ_1 and ρ_2. In general, $F(\rho_1, \rho_2) = (Tr\{\sqrt{\sqrt{\rho_1}\rho_2\sqrt{\rho_1}}\})^2$, which simplifies to $|\langle\psi_1 | . \psi_2\rangle|^2$ for pure states.
6. In comparison, in the typical 3° half-opening angle geometry, the relative polarizations are $86.9°_p$ and $93.2°_p$ from the first crystal (collected at azimuthal angles 0° and 180°) due to the Migdall effect (see Figure 3). Nevertheless, they are routinely employed in this configuration in the two-crystal scheme to produce high-fidelity maximally entangled states: the fidelity of $(|86.9_p°, 93.2_p°\rangle + |0_p°, 0_p°\rangle)/\sqrt{2}$ with $|\psi\rangle_{max}$ is 99.7%, with a predicted concurrence > 98%. Most experiments to date have not been sensitive to much minor imperfections.
7. To obtain the theory curves, the downconversion polarization from the second crystal was calculated using exactly the same parameters used for the first crystal, except the optic axis, which was rotated by 90°. Thus, strictly speaking, what we now call the azimuthal coordinate in the lab frame is the azimuthal coordinate defined with respect to the first crystal.
8. Collecting at unconventional azimuthal angles in the lab frame, e.g. 105° and 285°, would require a detection plane that is no longer parallel to the optical table, resulting in the need for complicated mounts and alignment. Therefore, instead of rotating the detection plane, we choose to rotate everything else, i.e. the pump polarization, crystal optic axis and the analyzing polarizers. Thus, the downconversion polarizations are relabeled, i.e. $105_p° \rightarrow 90_p°$.

References

[1] Migdall, A. *J. Opt. Soc. Am. B* **1997,** *14,* 1093–1098.

[2] Altepeter, J.; Jeffrey, E.; Kwiat, P. *Opt. Express* **2005**, *13*, 8951–8959; Erratum: Akselrod, G.M.; Altepeter, J.; Jeffrey, E.; Kwiat, P. *Opt. Express* **2007**, *15*, 5260–5261.

[3] Osorio, C.I.; Molina-Terriza, G.; Torres, J.P. *J. Opt. A: Pure Appl. Opt.* **2009,** *11,* 094013.

[4] U'Ren, A.; Banaszek, K.; Walmsley, I. *Quantum Inf. Comput.* **2003,** *3,* 480–502.

[5] Vincent, L.E.; U'Ren, A.B.; Rangarajan, R.; Osorio, C.I.; Torres, J.P.; Zhang, L.; Walmsley, I.A. *New J. Phys.*, in press, 2010.

[6] Rangarajan, R.; Vicent, L.E.; U'Ren, A.B.; Kwiat, P.G. *J. Mod. Opt.* **2011,** *58,* 318–327.

[7] Kwiat, P.G.; Waks, E.; White, A.G.; Appelbaum, I.; Eberhard, P.H. *Phys. Rev. A* **1999,** *60,* R773–R776.

[8] Wootters, W.K. *Phys. Rev. Lett.* **1998,** *80,* 2245–2248.

[9] Rangarajan, R.; Goggin, M.; Kwiat, P. *Opt. Express* **2009,** *17,* 18920–18933.